World Academy of Science, Engineering and Technology
International Journal of Materials and Metallurgical Engineering
Vol:11, No:1, 2017

Preparation and Conductivity Measurements of LSM/YSZ Composite Solid Oxide Electrolysis Cell Anode Materials

Christian C. Vaso, Rinlee Butch M. Cervera

Open Science Index, Materials and Metallurgical Engineering Vol:11, No:1, 2017 publications.waset.org/10006060.pdf

***Abstract*—**One of the most promising anode materials for solid oxide electrolysis cell (SOEC) application is the Sr-doped $LaMnO_3$ (LSM) which is known to have a high electronic conductivity but low ionic conductivity. To increase the ionic conductivity or diffusion of ions through the anode, Yttria-stabilized Zirconia (YSZ), which has good ionic conductivity, is proposed to be combined with LSM to create a composite electrode and to obtain a high mixed ionic and electronic conducting anode. In this study, composite of lanthanum strontium manganite and YSZ oxide, $La_{0.8}Sr_{0.2}MnO_3/Zr_{0.92}Y_{0.08}O_2$ (LSM/YSZ), with different wt.% compositions of LSM and YSZ were synthesized using solid-state reaction. The obtained prepared composite samples of 60, 50, and 40 wt.% LSM with remaining wt.% of 40, 50, and 60, respectively for YSZ were fully characterized for its microstructure by using powder X-ray diffraction (XRD), Thermogravimetric analysis (TGA), Fourier transform infrared (FTIR), and Scanning electron microscope/Energy dispersive spectroscopy (SEM/EDS) analyses. Surface morphology of the samples via SEM analysis revealed a well-sintered and densified pure LSM, while a more porous composite sample of LSM/YSZ was obtained. Electrochemical impedance measurements at intermediate temperature range (500-700 °C) of the synthesized samples were also performed which revealed that the 50 wt.% LSM with 50 wt.% YSZ (L50Y50) sample showed the highest total conductivity of $8.27x10^{-1}$ S/cm at 600 ºC with 0.22 eV activation energy.

***Keywords*—**Ceramics, microstructure, fuel cells, electrochemical impedance spectroscopy.

I. Introduction

THE use of green or renewable energy has received increasing interest in recent years in order to realize a sustainable low-carbon emission economy. Two of the most promising renewable energy sources are the solar energy and wind power and are most promising for replacing the existing fossil fuel-based energy sources. However, these energy sources are site-specific and intermittent, and thus are not reliable for continuous supply of energy. Although battery storage can solve the time mismatch between energy supply and demand, the low storage capacity and short equipment life of batteries limit the practical application of such an approach. One of the solutions is to transform these renewable energies into another form wherein one of the identified potential alternative fuel and energy carrier for future energy supplies is the hydrogen. In particular, the combination of hydrogen and fuel cells is expected to lead to new high-efficiency energy networks [1].

Hydrogen is a leading candidate as alternative future fuel. Currently, hydrogen is produced from fossil fuels by steam reforming, partial oxidation of methane, and gasification of coals which are non-renewable and pose negative impacts in the environment. Other means of producing hydrogen which are more environmentally friendly are by means of thermochemical water splitting and photocatalytic water splitting, but these production means have too low efficiency to be economically competitive [2]. Thus, efforts to produce hydrogen efficiently and sustainably without jeopardizing environmental concerns had led researchers to investigate SOEC as means to convert water into energy. Water electrolysis is one of most favored production processes for hydrogen generation. In line with this, high temperature electrolysis of steam (HTE), such as in SOEC, is expected to consume less electrical energy as compared to electrolysis at low temperature as consequence of the more favorable thermodynamic and electrochemical kinetic conditions for the reaction [3].

High-temperature SOEC has great potential for efficient and economical production of hydrogen fuel [4]. By splitting water in the form of steam, hydrogen can be efficiently derived from this ceramic based mechanism. However, degradation of the cell during operation still represents a scientific and technological barrier in view of its development at an industrial scale [5]. Main causes of degradation can be attributed to the formation of secondary phases and mechanical stress that leads to both non-ohmic and ohmic resistances. The most detrimental effect which is also the most widely reported in the literature is the delamination of the oxygen electrode [6].

To fully achieve the advantages of SOEC, it is necessary to synthesize electrodes that would effectively lengthen the operating time of SOECs. Particularly, the anode component of the SOEC must be chemically stable in highly reducing environments, must have good ionic and electronic conductivity, must have suitable porosity and pore size, and must have relatively close thermal expansion coefficient value with electrolyte material [7]. So far, the most common used anode materials are mixed oxides with perovskite structure, such as the LSM because of its close thermal expansion coefficient value with YSZ electrolyte. However, during

C. C. Vaso is with the Dept. of Engineering Science, College of Engineering and Agro-Industrial Technology, University of the Philippines Los Baños, Philippines.

R. B. Cervera is with the Advanced Ceramics Research Laboratory, Department of Mining, Metallurgical, and Materials Engineering, University of the Philippines Diliman, Quezon City, 1101 Metro Manila, Philippines (e-mail: rmcervera@up.edu.ph).

Open Science Index, Materials and Metallurgical Engineering Vol:11, No:1, 2017 publications.waset.org/10006060.pdf

operation, poor conducting compounds are formed in the interface of the LSM and the electrolyte (usually YSZ) [8], [9]. By creating a composite LSM-YSZ instead of a pure LSM, degradation is expected to be minimized while efficiently diffusing of oxide ions. Hence, in this study, composite samples of LSM-YSZ with different wt.% compositions have been synthesized and characterized as a potential anode material.

II. Experimental

A. Synthesis of LSM and YSZ Composite Materials

The starting materials in synthesizing lanthanum strontium manganite ($La_{0.8}Sr_{0.2}MnO_3$) are La_2O_3 (99.99%, TPC), MnO_2 (99%, UNILAB Reagents), and $SrCO_3$ (99.99%, Sigma-Aldrich), while for YSZ ($Zr_{0.92}Y_{0.08}O_2$) they are ZrO_2 (98%, High Purity Chemicals) and Y_2O_3 (99.9%, Sigma-Aldrich). The pure LSM and pure YSZ were first synthesized via solid state reactions with calcination at 1000 ºC for 6h and sintering at 1200 ºC for 12h. These prepared samples were then used to synthesize the composite samples with different wt.% of LSM and YSZ. To have a L50Y50 composite sample, which basically refers to 50% LSM and 50% YSZ by wt.%, 0.5 grams of LSM and 0.5 grams of YSZ were mixed and ground to produce 1 gram of L50Y50 composite sample. The ground samples were then oven dried, pelletized, and then sintered at 1150 °C for 5h. Same steps were taken for the other compositions, L60/Y40 and L40Y60.

B. Characterization

A representative precursor as-ground composite material was first analyzed for its thermal properties using TGA (SII TG/DTA 6300). The final sintered products were fully characterized for its microstructure using powder XRD, FTIR, SEM/EDS, and electrochemical impedance spectroscopy (EIS) measurements. XRD analysis was run on the samples using an X-ray diffractometer Siemens Kristalloflex 760 X-ray Generator with Cu-k_α tube with λ equal to 1.5406 Å. FT-IR analysis was performed using a Thermo Scientific Nicolet 6700 model. Morphological characteristics of the samples were investigated via SEM/EDS using a Hitachi SU3500 SEM model coupled with Thermo Noran System 7 EDS. For the conductivity measurements, a pelletized sample is formed into a rectangular shaped pellet using a diamond saw. The pellet is coated with silver paste and sandwich into two gold foils. A laboratory setup composed of a fabricated tube furnace, fuel cell holders, platinum interconnects, and an electrochemical workstation (BioLogic VMP-300) was utilized to conduct the measurement under oxygen at temperature range of 500 °C – 700 °C. Frequency range of 5 MHz to 1 mH was utilized during the course of the conductivity measurements.

III. Results and Discussion

The TGA of the as-ground representative precursor composite sample of 60 wt.% LSM and 40 wt.% YSZ, denoted as L60Y40, is shown in Fig. 1. The thermogram revealed three major weight losses which can be attributed to desorption of physisorbed and chemisorbed water below 300 °C, hydroxide decomposition at intermediate temperatures, and decomposition of carbonate precursor materials around 700-900 °C. The observed total wt.% loss up to 900 °C is about 9%. From this observation and result, the calcination temperature for all samples is set at 1000 °C wherein no more further large weight loss was observed.

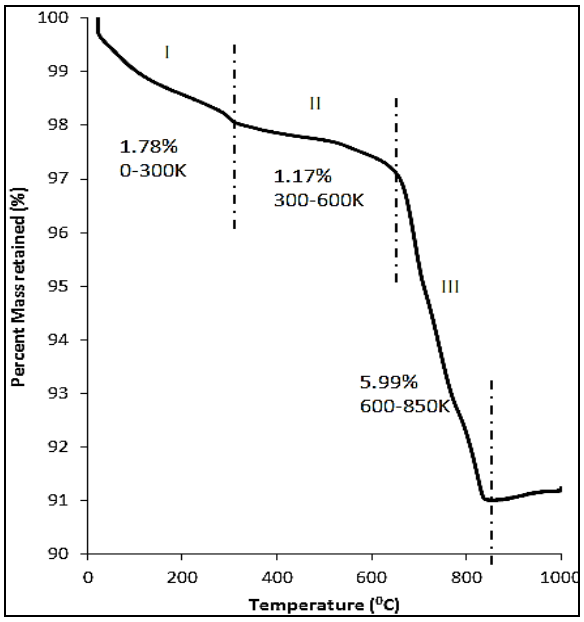

Fig. 1 TGA graph of L60Y40 as-prepared precursor sample

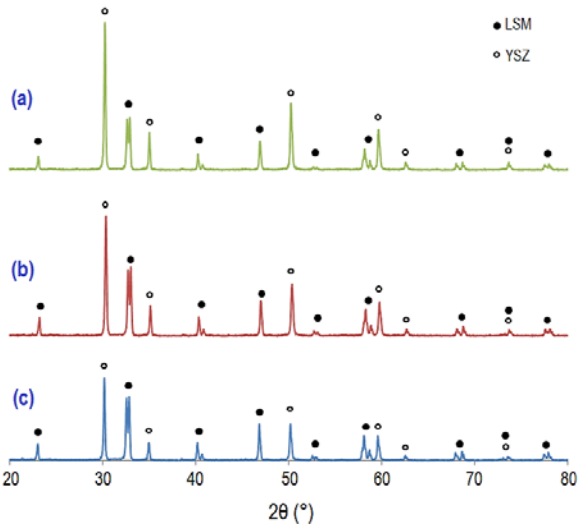

Fig. 2 XRD stack pattern of samples sintered at 1150 °C for 5h for (a) L40Y60, (b) L50Y50, (c) L60Y40

Fig. 2 shows the stacked powder XRD patterns of the synthesized different weight percent composition of LSM and YSZ. The diffraction peaks observed can be indexed to both distinct peaks of tetragonal LSM and cubic YSZ with no distinguishable impurity peaks. The splitting of the LSM peaks can be observed. The calculated lattice parameters for tetragonal LSM in L40Y60 are a =3.84 Å and c=7.63 Å and

Open Science Index, Materials and Metallurgical Engineering Vol:11, No:1, 2017 publications.waset.org/10006060.pdf

a=5.15 Å for the YSZ. These lattice parameters are similar for the other composite samples of L50Y50 and L60Y40.

The FTIR results for the functional group analysis of the prepared composite samples are shown in Fig. 3. The FITR results revealed that the samples contain no major organic species and O-H vibration bands [10], [11]. Vibration bands at 400 cm^{-1} to 800 cm^{-1} can be observed in the spectra which can be attributed to metal-oxygen-metal vibration bands in the sintered ceramics samples [12].

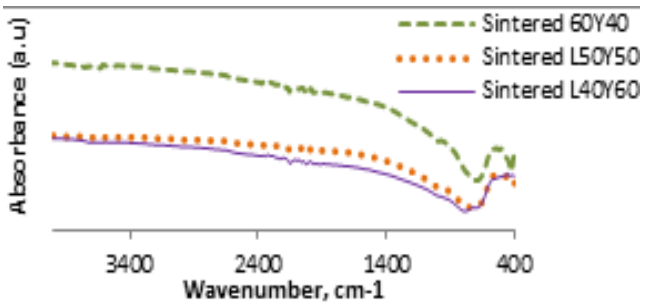

Fig. 3 FTIR graph of the different sintered LSM/YSZ samples

The obtained sintered samples were also subjected to surface morphology characterization by using SEM technique. Fig. 4 shows the SEM images for pure LSM (Fig. 4 (a)) and for the composite samples (Figs. 4 (b)-(d)). As can be observed from the images, a well sintered and densified sample is obtained for pure LSM with relative density of 94.5%. The morphology can be described as cubic and beveled-like microstructure. However, for the composite samples, a more porous morphology can be seen with relative densities of 84.8%, 82.8%, and 83.8% for L60Y40, L50Y50, and L40Y60, respectively. These porosities are needed for the enhanced electrochemical performance of the anode materials in the SOEC operation especially for the triple-phase anodic reaction. On the other hand, the elemental mapping for the distribution of elements in the prepared representative composite sample of L60Y40 is shown in Fig. 5. EDS analysis revealed good mixing of LSM and YSZ in the sample.

Fig. 6 shows the electrical conductivity measurements of the different prepared samples under oxygen gas flow environment at temperatures 500 to 700 °C. Pure LSM shows the highest conductivity reaching to 1.1 S/cm at 600 °C and activation energy of 0.16 eV. On the other hand, L50/Y50 has the highest total conductivity followed by L60Y40 and L40Y60 with activation energies of 0.22 eV, 0.33 eV, and 0.42 eV. The trend revealed that the 50/50 wt.% composition of LSM and YSZ showed the highest conductivity among the composite samples. The decrease in the total conductivity of L60/Y40 can be attributed to possibly low oxide-ion conductivity contribution of YSZ, while the low total conductivity of L40Y60 can be attributed to low electronic conductivity contribution of LSM and higher activation energy due to higher amount of YSZ. The total conductivities observed for L60/Y40, L50/Y50, and L40/Y60 are $5.01x10^{-1}$ S/cm, $8.27x10^{-1}$ S/cm, and $4.19x10^{-1}$ S/cm at 600 °C, respectively.

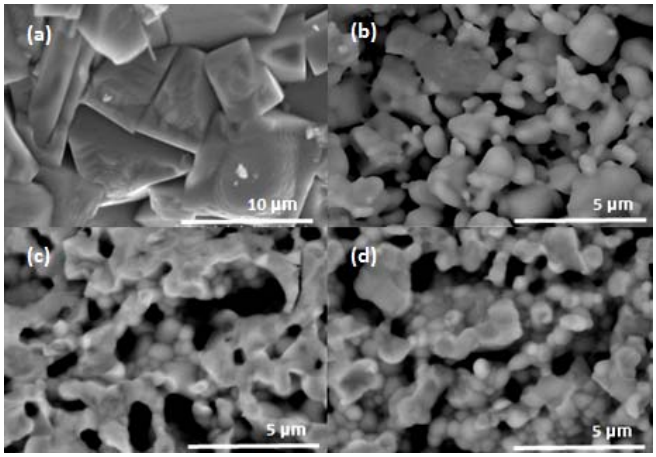

Fig. 4 SEM images of sintered samples for (a) pure LSM, (b) L60Y40, (c) L50Y50, (d) L40Y60

IV. Conclusion

Different wt.% ratio compositions of LSM and YSZ (L40Y60, L50Y50, L60Y40) were successfully prepared via solid-state reaction. The XRD patterns revealed some distinct peaks of LSM and YSZ at different prepared compositions which can be indexed to tetragonal LSM with lattice parameters of a =3.84 Å and c=7.63 Å and a=5.15 Å for cubic YSZ in all composite samples prepared. FTIR analysis showed no major organic impurity vibration bands, while SEM images revealed a porous microstructure of the composites samples. The EIS measurements for the total conductivity revealed that among the prepared composite samples, the L50Y50 showed the highest conductivity of $8.27x10^{-1}$ S/cm at 600 °C.

Open Science Index, Materials and Metallurgical Engineering Vol:11, No:1, 2017 publications.waset.org/10006060.pdf

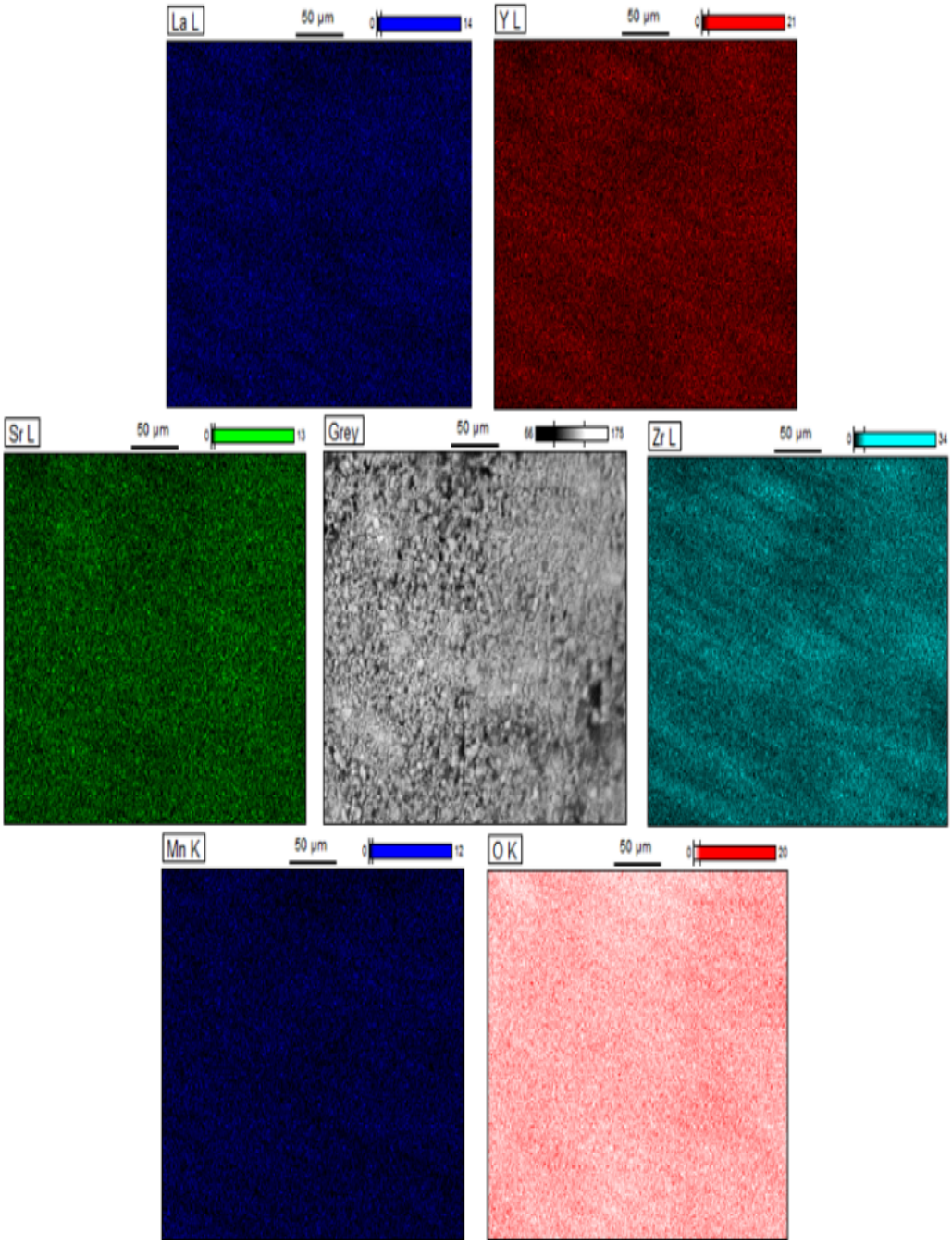

Fig. 5 SEM image (center) with EDS analyses of the L60Y40 sintered sample

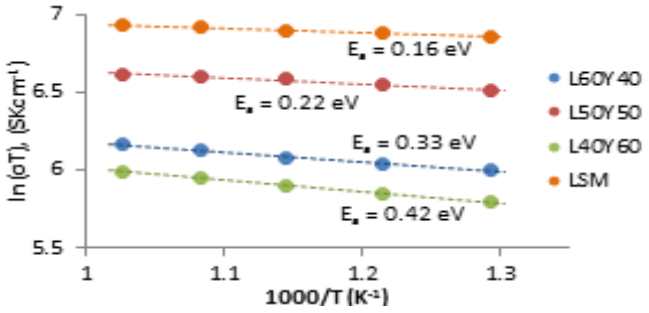

Fig. 6 Arrhenius-type plot of the total conductivity of the different sintered samples under O_2 gas flow environment

ACKNOWLEDGMENT

This study is financially supported by the Philippine-California Advanced Research Institute-Commission on Higher Education Institute (PCARI-CHED) for Information Infrastructure Development GREENPower research grant (IIID-2015-09) and in part by the Engineering Research and Development for Technology scholarship Department of Science and Technology (ERDT-DOST).

REFERENCES

[1] W. Wang et al., "A comparison of LSM, LSF and LSCo for Solid Oxide electrolyzer anodes", Journal of Electrochemical Society, 153(11), 2006, A2066-A2070.

[2] F. Suleman, I. Dincer, & M. Agelin-Chaab, "Environmental impact assessment and comparison of some hydrogen production options", International Journal of Hydrogen Energy, 40(21), 2015, 6976-6987.

[3] A. Brisse and P. Mocoteguy, "A review and comprehensive analysis of degradation mechanisms of solid oxide electrolysis cells", International Journal of Hydrogen Energy, 38, 2013, 15887-15902.

[4] P. Kazempoor P. and R.J. Braun, "Hydrogen and synthetic fuel production using high temperature solid oxide electrolysis cells (SOECs)", International Journal of Hydrogen Energy, 40(9), 2015, 3599-3612.

[5] A. Nechache and M. Cassir, A. ringuede, "Solid oxide electrolysis cell analysis by means of electrochemical impedance spectroscopy: A review", Journal of Power Sources, 258, 2014, 164-181.

[6] N. Li et al., "Mitigation of the delamination of LSM anode in Solid Oxide electrolysis cells using Manganese-modified Yttria-Stablized Zirconia", International Journal on Hydrogen Energy, 38(15), 2013, 6298-6303.

[7] M. Ni, Michael K.H. Leung, D. Leung, "Technological development of hydrogen production by Solid Oxide electrolyzer cell (SOEC)", International Journal of Hydrogen Energy, 33(9), 2008, 2337-2354.

[8] M. Keane, Manoj K. Mahapatra, Atul Verma 1, Prabhakar Singh, "LSM/YSZ interactions and anode delamination in solid oxide electrolysis cells", International Journal of Hydrogen Energy, 37(22), 2012, 16776-16785.

[9] E. Shin et al., "Polarization mechanism of high temperature electrolysis in a Ni-YSZ/YSZ/LSM solid oxide cell by parametric impedance analysis", Solid State Ionics, 232, 2013, 80-96.

[10] R. B. Cervera, et.al., "Perovskite-Structured BaScO2(OH) as a Novel Proton Conductor: Heavily Hydrated Phase Obtained via Low-Temperature Synthesis", Chem. Mater. 25, 2013, 1483-1489.

[11] R. B. Cervera, et.al., "Nanograined Sc-doped BaZrO3 as a proton conducting solid electrolyte for intermediate temperature solid oxide fuel cells (IT-SOFCs)", Solid State Ionics, 264, 2014, 1-6.

[12] M. B. Kakade, K. Bhattacharyya, R. Tewari, R. J. Kshirsagar, A. K. Tyagi, S. Ramanathan, G. P. Kothiyal & D. Das, "Nanocrystalline La0.84Sr0.16MnO3 and NiO-YSZ by Combustion of Metal Nitrate-Citric Acid/Glycine Gel – Phase Evolution and Powder Characteristics", Transactions of the Indian Ceramic Society, 72:3, 2013, 182-190.

Open Science Index, Materials and Metallurgical Engineering Vol:11, No:1, 2017 publications.waset.org/10006060.pdf